DOI: 10.1002/ejic.200501008

Peroxotungstates and Their Citrate and Tartrate Derivatives

Shu-Ya Hou,[a,b] Zhao-Hui Zhou,*[a] Tao-Ran Lin,[a] and Hui-Lin Wan[a]

Keywords: Bioinorganic chemistry / Peroxo ligands / Polyoxometalates / Tungsten

The reaction of potassium tungstate with the biologically relevant ligands citric and tartaric acid, in the presence of hydrogen peroxide, was investigated to discover the effect of pH variation on the product pattern. The reaction with citric acid led to the formation of the dimer $K_5[WO(O_2)_2(Hcit)H(Hcit)(O_2)_2OW]{\cdot}6H_2O$ (**1**; H_4cit = citric acid) due to carboxyl-carboxylic acid hydrogen bonding in the pH range 2–5; this complex can also be obtained by an exchange reaction between the oxo ligands of the dimeric hydrogencitrate tungstate $K_4[W_2O_5(Hcit)_2]{\cdot}4H_2O$ (**6**) and H_2O_2. Interestingly, a novel dimeric peroxotungstate $K_3[W_2O_3(O_2)_4(OH)]{\cdot}H_2O$ (**2**), without the coordination of citrate ligands, was isolated in the pH range 7–9, as confirmed by ^{17}O NMR solution studies. The reaction of potassium tungstate with (*R*,*R*)-tartaric acid afforded the tartratoperoxotungstate $K_4[W_2O_2(O_2)_4\{(R,R)\text{-tart}\}]{\cdot}3H_2O$ [**3**; H_4tart = (*R*,*R*)-tartaric acid] in the pH range 1–3. The dimeric peroxotungstate $K_2[W_2O_3(O_2)_4(H_2O)_2]{\cdot}2H_2O$ (**4**) was found to react with citric or tartaric acid at pH 2–5 or 2–3, respectively, to give species **1** and **3**. Evidence that **1** exists as a dimer in solution is presented. The three complexes were characterized by elemental analysis, IR and NMR spectroscopy, and X-ray structural analyses. The formation of these complexes is dictated by pH, and the thermal stabilities of **1** and **3** vary with the coordinated ligands.
(© Wiley-VCH Verlag GmbH & Co. KGaA, 69451 Weinheim, Germany, 2006)

Introduction

Due to their catalytic activity and specialized redox behavior, peroxotungstates have received special attention in a variety of industrial, pharmaceutical, and biological processes as they can be regarded as an environmentally friendly alternative to traditional oxidation reactions that represents an improvement in terms of pollution prevention.[1] They are widely used in stoichiometric as well as catalytic oxidation in organic chemistry,[2] for example in the oxidation of alcohols,[3,4] internal alkenes,[5] amines,[6] sulfides,[4,7,8] isobutyraldehyde,[9] hydroquinones,[2] bromide,[10] benzyl chlorides,[11] epoxidation of chiral allylic alcohols,[12] geraniol, linalool[13] and also in olefin epoxidations,[14–17] such as cyclohexene,[18] propylene,[19] alkene,[20] and *cis*-1-propenylphosphonic acid.[21] To better understand these catalytic processes, a more detailed characterization of peroxotungstates is necessary. It appears that $[W(O_2)_4]^{2-}$ predominates at high pH (>7) and in the presence of excess H_2O_2,[22] whereas at intermediate pH (1.3–7.0) the dimer $[W_2O_3(O_2)_4(H_2O)_2]^{2-}$ is the major species,[23] and at lower pH the solution become unstable and lose oxygen.[24] Although other peroxotungstates have also been observed in the solid state[25–27] and solution,[28,29] the key to stabilizing peroxotungstates is to incorporate a ligand that can effectively coordinate to tungsten. The reactivity of peroxo complexes also depends on both the number and nature of the auxiliary ligands.

A variety of peroxotungstates with oxygen and nitrogen donors have been studied in solution and in the solid state.[28–39] However, unlike peroxomolybdates(VI), which have been investigated extensively,[40–47] fewer peroxotungstate species with other ligands have been structurally reported. Known compounds include dimeric oxalate and tetranuclear carbonate complexes such as $M_2[WO(O_2)_2(C_2O_4)]$ ($M = K^+$, NH_4^+)[48,49] $[(n\text{-}C_4H_9)_4N]_2[W_2O_2(O_2)_4(C_2O_4)]$,[50] $K_6[W_4O_8(O_2)_6(CO_3)]{\cdot}6H_2O$,[51] or isoperoxotungstates like $K_2[W(O_2)_4]$,[22] $K_2[W_2O_3(O_2)_2(H_2O)_2]{\cdot}2H_2O$,[23] $(Me_3CNH_3)_4[W_4O_{12}(O_2)_2]$,[25] $[(n\text{-}C_4H_9)_4N]_2[W_4O_6(O_2)_6(OH)_2(H_2O)_2]{\cdot}H_2O$,[26] and $Cs_2(CN_3H_6)_3[(C_2H_5)_2NH_2][W_7O_{22}(O_2)_2]{\cdot}3H_2O$.[27]

Citrate ions are present in most plant and animal tissues where they regulate various fundamental physiological processes and are intermediates in carbohydrate metabolism, such as in the Krebs cycle. (*R*,*R*)-Tartaric acid, which is also widely distributed in nature and is classified as a fruit acid, is another example of an α-hydroxycarboxylic acid that is involved in many biochemical processes. Our study in this field has been undertaken in order to answer one fundamental question, namely whether a pH variation can act as the sole factor to induce structural changes in isolable peroxotungstates in a hydrogen peroxide solution containing both tungstate and citrate or tartrate ions. It should be

---

[a] Department of Chemistry, College of Chemistry and Chemical Engineering and State Key Laboratory of Physical Chemistry of Solid State Surfaces, Xiamen University,
Xiamen 361005, China
[b] College of Chemistry and Chemical Engineering, Donghua University,
Shanghai 201620, China
Fax: +86-592-218-3047
E-mail: zhzhou@xmu.edu.cn

Supporting information for this article is available on the WWW under http://www.eurjic.org or from the author.

noted that peroxotungstates are much more unstable and their isolation is more difficult than their peroxomolybdate homologs.

Here we report the isolation and characterization of the dimeric citrato and tartrato peroxotungstates $K_5[WO(O_2)_2(Hcit)H(Hcit)(O_2)_2OW]\cdot 6H_2O$ (**1**) and $K_4[W_2O_2(O_2)_4\{(R,R)\text{-tart}\}]\cdot 3H_2O$ (**3**). The hydroxy-bridged dinuclear peroxotungstate $K_3[W_2O_3(O_2)_4(OH)]\cdot H_2O$ (**2**) was also isolated serendipitously from a weakly basic solution and is the first example of an isolated dimeric $W_2O_3(O_2)_4(OH)$ skeleton.

Results and Discussion

Scheme 1 shows the different pathways that lead to peroxo compounds **1**–**4**. The compound numbers shown correspond both to the potassium salts and the anions of the complexes, which are used interchangeably in this description. It appears that pH acts as a decisive factor in dictating the structural features of the isolated complexes. When the pH of an aqueous solution containing potassium tungstate, potassium citrate, and excess hydrogen peroxide was adjusted to 2–5, the dimer **1** was isolated, and this compound could also be isolated by the treatment of **4** with citric acid under comparable conditions. The dimeric peroxotungstate **4** is in equilibrium with the monomeric species in aqueous solution,[29] and it is possible that the monomeric species reacts directly with the citrate or tartrate to form **1** or **3**. Alternatively, complex **1** was prepared at pH 4 by the reaction of H_2O_2 with the dimeric hydrogencitratodioxotungstate $K_4[W_2O_5(Hcit)_2]\cdot 4H_2O$ (**6**), which was isolated from a solution of potassium tungstate and citric acid at pH 3.0–3.5. This is a clear demonstration that the β-carboxylate in complex **6** is relative weakly coordinated and can be detached by a peroxo group, which results in the formation of a more stable didentate citrate peroxotungstate at pH 2–5.

It is significant that **1** is a centrosymmetric dimer formed through the linear hydrogen bonding of a β-carboxy to a β-carboxylic acid group [O···O = 2.502(8) Å]. In view of the intramolecular hydrogen-bonding distance [O···O = 2.636(7) Å] in salicylic acid,[52] and the ordinary OH bond of 0.96 Å, the hydrogen bonding in **1** must be very strong as an intramolecular mode. This, in turn, reveals the stability of dimer **1**. In light of its low solubility and its ^{13}C and ^{1}H NMR signals, which will be discussed later, **1** probably exists as a dimer both in the crystalline state and in solution due to this strong hydrogen bonding.

When the pH of the same solution that formed **1** was changed to 7–8, it slowly deposited $K_2[W_2O_3(O_2)_4(OH)]\cdot H_2O$ (**2**) instead of the molybdate(VI) analog $[WO(O_2)_2(cit)]^{4-}$ (**5**).[45] Here, citric acid acts as both reactant and buffer

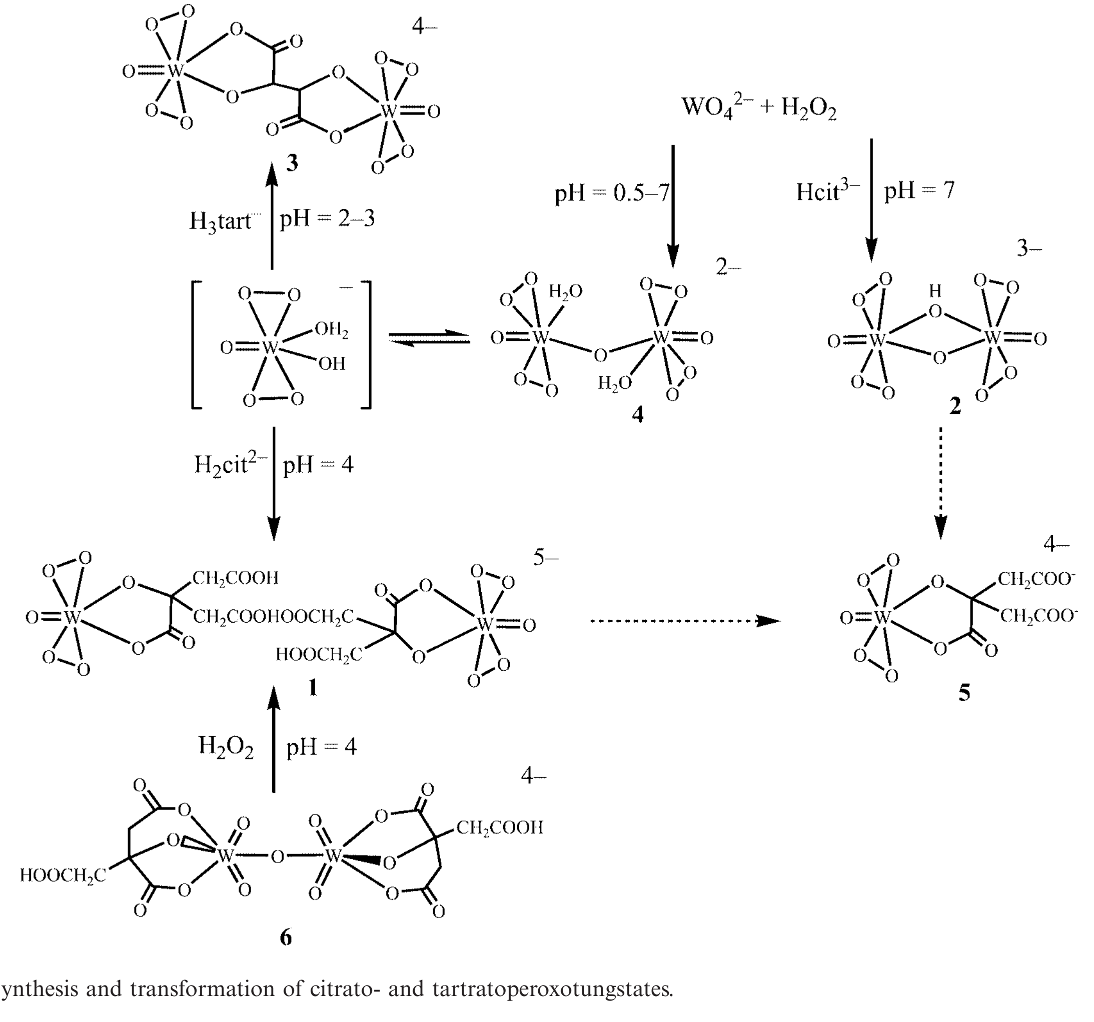

Scheme 1. Synthesis and transformation of citrato- and tartratoperoxotungstates.

agent to capture this species. As the pH value increases, the coordination ability of citrate with peroxotungstate decreases and therefore complex **5** is not isolated. Reversible dimerization and dissociation do not occur. It is known that the monomeric species $[W(O_2)_4]^{2-}$ is the principal species at high pH (7–9) in the presence of excess H_2O_2,[22] while the dimeric anion $[W_2O_3(O_2)_4(H_2O)_2]^{2-}$ (**4**) is the major species at intermediate pH (1.3–7.0). Complex **2** could be an intermediate between the two peroxotungstates mentioned above, and it can also be considered as the product of deprotonation of the coordinated water molecule in $K_2[W_2O_3(O_2)_4(H_2O)_2]\cdot 2H_2O$ (**4**). Complex **4** exhibits high catalytic activity for the epoxidation of various allylic alcohols using hydrogen peroxide in water.[53]

The pH is also critical in the formation of the tartratoperoxotungstate **3**. The reaction of potassium tungstate, (*R*,*R*)-tartaric acid, and excess hydrogen peroxide in aqueous solution at pH 2–3 gave **3**, which can also be obtained by treating **4** with (*R*,*R*)-tartaric acid under comparable conditions via the monomeric peroxo species. The higher pH only led to the formation of potassium tartrate. Complex **3** is efflorescent, and can easily be converted into a powder by dehydration.

An equilibrium between dimeric and monomeric peroxotungstate species like $[WO(O_2)_2(OH_2)]$ and $[W_2O_3(O_2)_4(H_2O)_2]^{2-}$ has been proposed,[28,29] therefore it does not seem necessary that **1** and **3** are directly formed from **4**. Although the detailed structures of the monomeric peroxotungstates remain controversial,[32] some monomeric species like $[WO(O_2)_2(OH_2)_2]$, $[WO(O_2)_2(OH)(OH_2)]^-$, $[WO(O_2)_2(OH)_2]^{2-}$, and $[WO(O_2)(OH)_3(OH_2)]$ are suggested.

Selected bond lengths and angles for the three compounds are summarized in Table 1, and further crystallographic data can be found in the Experimental Section. The structure of the anion in complex **1** is shown in Figure 1. Each tungsten atom is seven-coordinate with a pentagonal-bipyramidal geometry. The axial positions are occupied by the oxo ligand and the oxygen atom from an α-carboxy group. The equatorial positions are occupied by the two bonded peroxo groups and a deprotonated α-alkoxy group. The didentate (η^2-O_2^{2-}) ligand is a π-donor-like oxo ligand,[30] thus each peroxo and oxo ligand in this complex are in the *cis* configuration and interact with different metal orbitals. The citrate ion acts as a didentate ligand with the α-alkoxy and α-carboxy oxygen coordinated to the tungsten atom, while one of the β-carboxy groups is free to bind as a centrosymmetric dimer through a linear $[CO_2^-\cdots HO_2C]$ hydrogen bond, that is, one of the β-carboxylates of the citrate unit is bonded to the β-carboxylic acid group of the other unit.

Table 1. Selected bond lengths [Å] and angles [°] for $K_5[WO(O_2)_2(Hcit)H(Hcit)(O_2)_2OW]\cdot 6H_2O$ (**1**), $K_3[W_2O_3(O_2)_4(OH)]\cdot H_2O$ (**2**), and $K_4[W_2O_2(O_2)_4\{(R,R)\text{-tart}\}]\cdot 3H_2O$ (**3**).

Complex **1**					
W(1)–O(1)	2.015(3)	W(1)–O(2)	2.190(4)	W(1)–O(8)	1.707(4)
W(1)–O(9)	1.971(4)	W(1)–O(10)	1.926(4)	W(1)–O(11)	1.927(4)
O(1)–W(1)–O(2)	74.2(1)	O(1)–W(1)–O(8)	92.0(2)	O(1)–W(1)–O(9)	89.9(2)
O(1)–W(1)–O(10)	133.7(2)	O(1)–W(1)–O(11)	134.0(2)	O(1)–W(1)–O(12)	89.9(2)
O(2)–W(1)–O(8)	166.2(2)	O(2)–W(1)–O(9)	81.7(2)	O(2)–W(1)–O(10)	87.2(2)
O(2)–W(1)–O(11)	87.3(2)	O(2)–W(1)–O(12)	81.2(2)	O(8)–W(1)–O(9)	99.1(2)
O(8)–W(1)–O(10)	103.2(2)	O(8)–W(1)–O(11)	102.4(2)	O(8)–W(1)–O(12)	98.6(2)
O(9)–W(1)–O(10)	44.9(2)	O(9)–W(1)–O(11)	129.3(2)	O(9)–W(1)–O(12)	162.3(2)
O(10)–W(1)–O(11)	85.4(2)	O(10)–W(1)–O(12)	129.3(2)	O(11)–W(1)–O(12)	45.1(2)
O(6)···O(6)[a]	2.502(8)				
Complex **2**					
W(1)–O(1)	1.964(9)	W(1)–O(2)	1.933(8)	W(1)–O(3)	1.980(8)
W(1)–O(4)	1.947(7)	W(1)–O(5)	1.730(8)	W(1)–O(6)	2.219(6)
O(1)–W(1)–O(2)	45.3(3)	O(1)–W(1)–O(3)	163.0(3)	O(1)–W(1)–O(4)	131.0(3)
O(1)–W(1)–O(5)	98.6(4)	O(1)–W(1)–O(6)	81.7(3)	O(1)–W(1)–O(7)	90.6(4)
O(2)–W(1)–O(3)	129.8(3)	O(2)–W(1)–O(4)	86.5(3)	O(2)–W(1)–O(5)	102.1(4)
O(2)–W(1)–O(6)	86.3(3)	O(2)–W(1)–O(7)	134.5(4)	O(3)–W(1)–O(4)	44.6(3)
O(3)–W(1)–O(5)	98.4(4)	O(3)–W(1)–O(6)	81.7(3)	O(3)–W(1)–O(7)	88.3(4)
O(4)–W(1)–O(5)	100.5(4)	O(4)–W(1)–O(6)	87.6(3)	O(4)–W(1)–O(7)	131.9(4)
O(5)–W(1)–O(6)	168.5(3)	O(5)–W(1)–O(7)	94.2(4)	O(6)–W(1)–O(7)	74.3(3)
Complex **3**					
W(1)–O(1)	1.964(7)	W(1)–O(2)	2.224(8)	W(1)–O(4)	1.969(7)
W(1)–O(5)	1.928(8)	W(1)–O(6)	1.919(9)	W(1)–O(7)	1.996(9)
O(1)–W(1)–O(2)	76.1(3)	O(1)–W(1)–O(4)	89.7(3)	O(1)–W(1)–O(5)	132.1(4)
O(1)–W(1)–O(6)	134.8(4)	O(1)–W(1)–O(7)	90.0(4)	O(1)–W(1)–O(8)	95.9(4)
O(2)–W(1)–O(4)	82.3(4)	O(2)–W(1)–O(5)	85.3(4)	O(2)–W(1)–O(6)	86.0(4)
O(2)–W(1)–O(7)	80.5(4)	O(2)–W(1)–O(8)	171.9(4)	O(4)–W(1)–O(5)	43.8(4)
O(4)–W(1)–O(6)	129.0(4)	O(4)–W(1)–O(7)	162.4(4)	O(4)–W(1)–O(8)	98.7(5)
O(5)–W(1)–O(6)	86.0(4)	O(5)–W(1)–O(7)	130.2(4)	O(5)–W(1)–O(8)	101.0(4)
O(7)–W(1)–O(8)	98.8(5)	O(6)–W(1)–O(7)	45.8(4)	O(6)–W(1)–O(8)	99.4(5)

[a] Symmetry transformation: 1 – *x*, 1 – *y*, –*z*.

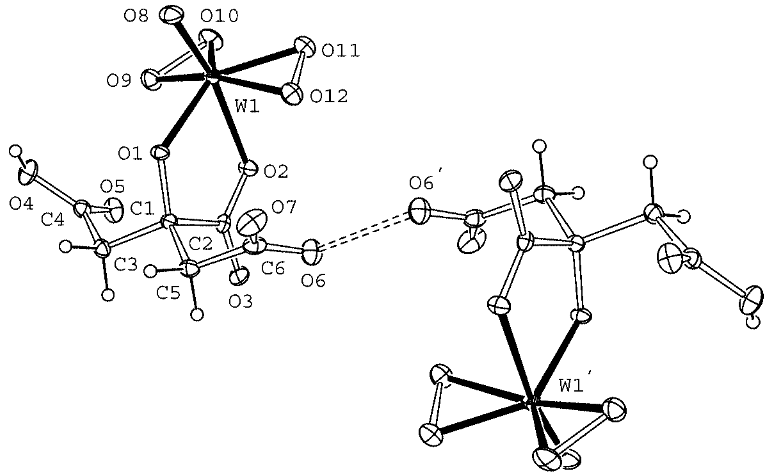

Figure 1. Perspective view of the anion structure of $K_5[WO(O_2)_2(Hcit)H(Hcit)(O_2)_2OW]\cdot 6H_2O$ (**1**).

As shown in Table 1, the W–O distances in complex **1** vary systematically. The distance of the W=O double bond is 1.707(4) Å, and the W–O(peroxo) bond lengths are in the range 1.927(4)–1.976(4) Å, which suggests that they are bonded asymmetrically. The slightly shorter W–O(alkoxy) bond [2.015(3) Å] indicates the deprotonation of the hydroxy group. The W–O(carboxy) bond is the longest [2.190(4) Å] due to the strong *trans* influence of the terminal oxo group.

An ORTEP diagram of the anion of **2** is shown in Figure 2. The dimeric complex **2** has a *cis* configuration and is bridged by two oxygen atoms. The existence of such a dimeric anion has been predicted previously by an ^{17}O NMR study.[28,29] The structure of **2** shows that one of the two bridged oxygen atoms is protonated, which represents a new isolated structural example of peroxotungstates. The coordination about the tungsten is essentially pentagonal bipyramidal. The equatorial place is defined by the five oxygen atoms corresponding to the two peroxo groups and one bridging oxygen atom. None of the atoms deviate more than 0.08 Å from the mean plane, and the tungsten atom is placed 0.23 Å above this plane. The axial positions are occupied by the oxo ligand and the hydroxy group. As shown in Table 1, the W–O6(hydroxy) bond [2.219(6) Å] is longer than the W–O7 bridge bond. The ligand binding is inferred to be significantly weaker at the axial position than the equatorial position due to the *trans* influence of the terminal oxygen.

The X-ray structure of the (*R*,*R*)-tartratoperoxotungstate **3** consists of discrete anions, potassium cations, and water molecules. As shown in Figure 3, the two $WO(O_2)_2$ moieties are spanned by a tartrato ligand that is didentate at each end, giving a pentagonal-bipyramidal coordination at the tungsten atoms. The tungsten is bound by a terminal oxo group, two didentate peroxo groups, and a didentate tartrate ligand that binds through its α-alkoxy and α-carboxy groups. The axial positions are occupied by the terminal oxo ligand [W–O = 1.707(9) Å] and an oxygen atom from the deprotonated carboxy group [W–O(2) = 2.224(8) Å]. The equatorial positions are occupied by the two slightly asymmetrically bound peroxo ligands, while the α-alkoxy group of the tartrate makes up the distorted pentagon [W–O = 1.964(7) Å]. It appears that the α-alkoxy group assumes the equatorial rather than the axial position so as to form a strong bond. The W–O(peroxo) distances in **3** vary only slightly. The W–O_2, W=O, and O–O distances in the peroxo groups are all within the range of distances previously observed for this class of peroxo complexes. Moreover, the potassium ions in complexes **1**–**3** are coordinated by water molecules, the oxygen atoms of the peroxo groups, and citrate or tartrate ligands. The coordination numbers of the potassium ions are between 7 and 9 and the coordination bond lengths of K–O between 2.65–3.30 Å. These ions are important for the stabilities of the overall structures: replacing the counterion with Na^+ results in no isolation of peroxotungstates **1**–**3**, which suggests that the sodium salt is more soluble in water than the potassium salt.

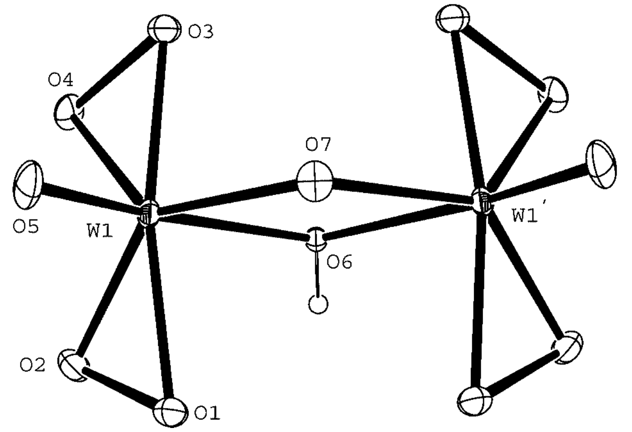

Figure 2. Perspective view of the anion structure of $K_3[W_2O_3(O_2)_4(OH)]\cdot H_2O$ (**2**).

Table 2 shows a comparison of Mo–O and W–O distances. The W–O distances of α-alkoxy group in the peroxotungstates are longer than those in their molybdate homologs, although the W–O distances of the α-carboxy groups are shorter than the Mo–O distances of the α-carboxy group.

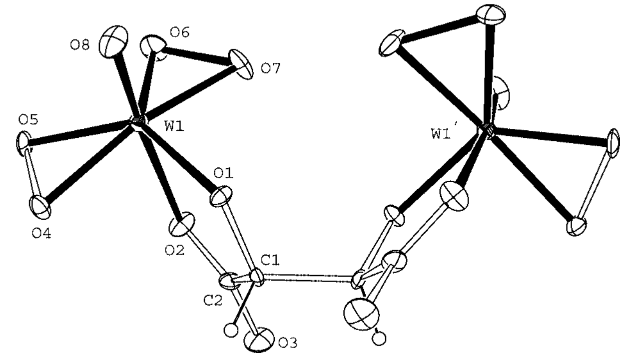

Figure 3. Perspective view of the anion structure of $K_4[W_2O_2(O_2)_4\{(R,R)\text{-tart}\}]\cdot 3H_2O$ (**3**).

O–O bond activation is a major feature of the reactivity of peroxo complexes, therefore it is instructive to compare the O–O distances in peroxotungstates and peroxomolybdates. The peroxo bonds in tungstates are slightly longer than those in molybdates, which indicates that activation of the peroxo group is much more effective with the peroxotungstates.

Complexes **1** and **3** display characteristic features of the coordinated citrate or tartrate ligand in their IR spectra. The coordinated carboxy frequencies are shifted to lower values compared to those of the free ligands. Specifically, absorptions for the antisymmetric stretching carboxy vibrations ν_{as}(COOH) and/or ν_{as}(COO) appear at 1731 and 1654 cm^{-1} for **1** and 1642 and 1612 cm^{-1} for **3**, and those of the symmetric stretching vibrations ν_s(COO) appear at 1440–1330 cm^{-1}. For the peroxotungstates without a carboxy ligand there is an obvious band at 703 or 763 cm^{-1}, which is assigned to the W–O–W vibration for **2** or **4**, respectively. The W=O vibrations appear as strong bands at 950/970, 928, and 947 cm^{-1} for **1**–**3**, respectively. The ν(O–O) vibration appears as a clearly defined strong band at around 840 cm^{-1}, which is a higher frequency than in the spectra of simple peroxide salts (800 cm^{-1}). Additional bands in the range 650–560 cm^{-1} belong to ν_{as}W(O–O) and ν_sW(O–O).

Owing to their dissociation on dissolution in H_2O (D_2O) the NMR spectra of **1** and **3** show additional peaks, although the major peaks could be interpreted. The ^{13}C NMR spectrum of $K_5[WO(O_2)_2(Hcit)H(Hcit)(O_2)_2OW]\cdot 6H_2O$ (**1**) displays four groups of resonance, with two close signals for each group. Complex **1** shows large low-field shifts of some ^{13}C resonances upon coordination relative to the corresponding carbons in the KH_3cit ion at a similar pH (3.4). For example, the shifts of the α-alkoxy carbons at δ = 88.1 and 85.6 ppm are 14.5 and 12 ppm, respectively, and those of the α-carboxy carbons at δ = 189.0, 187.4 ppm are 11.4 and 9.8 ppm, respectively (Figure 4). It also shows several AB quartets for the methylene protons of the coordinated citrate ligand in the ^1H NMR spectrum. The proton of the methylene belonging to the β-carboxy that forms hydrogen bonds is shifted to lower field than the others. These data do not conflict with the existence of **1** as a dimer in solution.

In the tartrate complex $K_4[W_2O_2(O_2)_4((R,R)\text{-tart})]\cdot 3H_2O$ (**3**), two singlets appear at around δ = 186 and 88 ppm in the ^{13}C NMR spectrum due to the α-carboxy and α-alkoxy groups. These low-field shifts relative to (*R*,*R*)-tartaric acid (δ = 177.1 and 72.0 ppm) imply the involvement of coordination (Figure 5). These results prove that the tartrate serves as a tetradentate ligand to form a dinuclear complex. The ^1H NMR spectrum of **3** shows multiple signals around δ = 5.3 ppm. These shifts occur at lower fields than in the free ligand. When these complexes are dissolved in D_2O they emit bubbles, thus the ^1H and ^{13}C NMR spectra display several additional peaks derived from the liberated ligand in addition to the signals of the complexes themselves.

Thermogravimetric (TG) and differential thermal analysis (DTA) were carried out for **1**–**4** under N_2; they indicated that the different ligands in the peroxo complexes give dif-

Table 2. A comparison of M–O (M = Mo, W) and O–O distances [Å] of peroxomolybdates and peroxotungstates.

Complex	M–O(α-alkoxy)	M–O(α-carboxy)	$M–O_{av}$ (peroxo)	O–O (peroxo)	Ref.
$K_2[MoO(O_2)_2(glyc)]\cdot 2H_2O$	1.991(5)	2.239(6)			[42]
$(NH_4)_2[MoO(O_2)_2(glyc)]\cdot 0.5EtOH$	1.974(2), 2.011(2)	2.211(2), 2.310(2)	1.962(2)	1.484(2)	[45]
$K_2[MoO(O_2)_2(H_2cit)]\cdot 3H_2O\cdot 0.5H_2O_2$	2.011(7)	2.220(8)	1.951(9)	1.48(1)	[41]
$K_2[MoO(O_2)_2(S\text{-}Hmal)]\cdot H_2O$	2.013(5)	2.281(4)	1.956(4)	1.492(7)av	[46]
$K_4[MoO(O_2)_2(cit)]\cdot 4H_2O$	1.971(2)	2.228(2)	1.959(2)	1.478(3)	[46]
$K_4[Mo_2O_2(O_2)_4\{(R,R)\text{-tart}\}]\cdot 4H_2O$	1.962(7)	2.248(7)	1.956(8)	1.48(1)	[43]
$K_4[W_2O_2(O_2)_4\{(R,R)\text{-tart}\}]\cdot 3H_2O$	1.964(7)	2.224(8)	1.953(9)	1.49(1)av	[a]
$K_5[MoO(O_2)_2(Hcit)H(Hcit)(O_2)_2OMo]\cdot 6H_2O$	2.033(5)	2.196(3)	1.953(3)	1.480(4)	[46]
$K_5[WO(O_2)_2(Hcit)H(Hcit)(O_2)_2OW]\cdot 6H_2O$	2.015(3)	2.190(4)	1.950(4)	1.494(6)	[a]
$K_6[W_4O_8(O_2)_6(CO_3)]\cdot 6H_2O$		2.18(2)	1.95(3)	1.48(5)	[51]
$(NH_4)_2[MoO(O_2)_2(C_2O_4)]$		2.045(3),2.261(3)	1.937(5)	1.475(4)	[45]
$[(n\text{-}C_4H_9)_4N]_2[WO(O)_2(C_2O_4)WO(O_2)_2]$		2.09(2), 2.40(1)	1.92(1)	1.48(2)	[50]
$K_2[MoO(O_2)_2(C_2O_4)]$		2.17(1)	1.95(1)	1.46(2)	[40]
$K_2[WO(O_2)_2(C_2O_4)]$		2.033(6), 2.245(6)	1.951(8)	1.51(1)	[48]
$K_2[Mo_2O_3(O_2)_4(H_2O)_2]\cdot 2H_2O$			1.968(1)	1.48(2)	[55]
$K_2[W_2O_3(O_2)_4(H_2O)_2]\cdot 2H_2O$			1.96	1.50	[23]
$K_2[W_2O_3(O_2)_4(OH)]\cdot H_2O$			1.956(9)	1.50(1)	[a]
$(Me_3CNH_3)_4[Mo_4O_{12}(O_2)_2]$			2.224(3)	1.473(4)	[25]
$(Me_3CNH_3)_4[W_4O_{12}(O_2)_2]$			2.233(6)	1.47(1)	[25]

[a] This work.

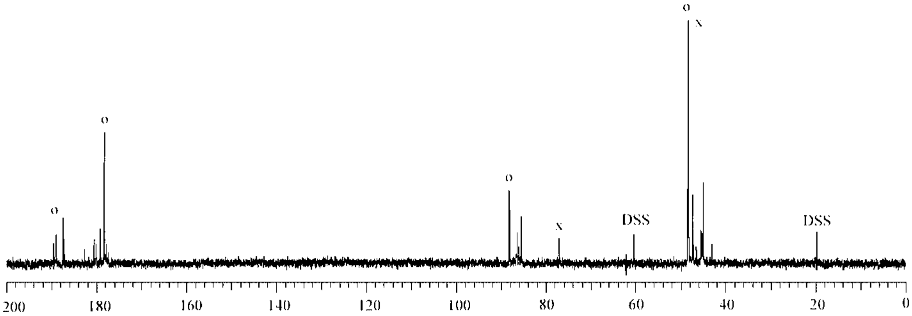

Figure 4. ^{13}C NMR spectra of the citratoperoxotungstate $K_5[WO(O_2)_2(Hcit)H(Hcit)(O_2)_2OW]\cdot 6H_2O$ (**1**). Labels: (x) free citrate; (o) coordinated citrate complex.

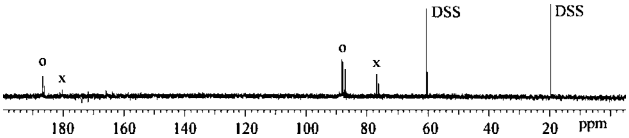

Figure 5. ^{13}C NMR spectra of the tartratoperoxotungstate $K_4[W_2O_2(O_2)_4\{(R,R)\text{-tart}\}]\cdot 3H_2O$(**3**). Labels: (x) free tartrate; (o) coordinated tartrate complex.

ferent thermal stability. The first decomposition in $K_5[WO(O_2)_2(Hcit)H(Hcit)(O_2)_2OW]\cdot 6H_2O$ (**1**), which is an endothermic process occurring at 112 °C, is believed to be associated with the loss of three H_2O molecules, and is followed by the loss of another three H_2O and peroxo groups at 166 °C. It is probable that **1** undergoes complete dehydration at this temperature and that this is followed by the rearrangement of the crystal lattice through an exothermic process, as confirmed by the TG and DTA plots, to form an anhydrous species such as $K_5[WO_3(Hcit)H(Hcit)O_3W]$. It then undergoes extensive decomposition at 301 °C to form potassium tungstate and carbonaceous matter due to the combustion of the citrate groups. The observed decomposition temperatures for the dehydration and decomposition of the peroxo groups of **1** are lower than for the corresponding Mo analogues, which may be related to the electrostatic interaction between M^{6+} and O_2^{2-}.

The dimeric peroxotungstate $K_2[W_2O_3(O_2)_4(OH)]\cdot H_2O$ (**2**) dehydrates in air and no water-loss step is observed. It is stable up to 158 °C, where it loses two peroxo groups. $K_4[W_2O_2(O_2)_4((R,R)\text{-tart})]\cdot 3H_2O$ (**3**) is not particularly stable and decomposes at 108 and 138 °C in exothermic processes that correspond to the loss of three water molecules and the loss of peroxo groups, respectively. $K_2[W_2O_3(O_2)_4(H_2O)_2]\cdot 2H_2O$ (**4**) first loses H_2O at 114 °C and then begins to lose its peroxo groups at 145 °C. These four complexes all showed rearrangement with exothermic process around 380 – 390 °C. From the data above, it is concluded that complexes **1** and **2** are much stable.

Experimental Section

Physical Measurements: Infrared spectra were recorded as Nujol mulls between KBr plates with a Nicolet 360 FT-IR spectrometer. Elemental analyses were performed with an EA 1110 elemental analyzer. ^1H and ^{13}C NMR spectra were recorded in D_2O on a Varian UNITY 500 NMR spectrometer using DSS (sodium 2,2-dimethyl-2-silapentane-5-sulfonate) as the internal reference. Thermogravimetric (TG) and differential thermal analysis (DTA) were carried out using a Netzsch Sta 449C thermal analyzer.

All experiments were carried out in the open air. All chemicals were analytical-grade reagents and were used without further purification. Nanopure-quality water was used throughout this work.

Preparation of $K_5[WO(O_2)_2(Hcit)H(Hcit)(O_2)_2OW]\cdot 6H_2O$ (1): Potassium tungstate, prepared from the reaction of tungsten trioxide (0.92 g, 4.0 mmol) and potassium hydroxide (2 M, 9 mL), was added dropwise to a solution containing citric acid (0.93 g, 4.4 mmol) and an excess of 30% hydrogen peroxide (1 mL). The resulting reaction mixture was adjusted to pH 4 with hydrochloric acid solution (1 M) in an ice-bath. Colorless crystals deposited gradually from the solution after several days in a refrigerator. They were collected and washed with ethanol to give **1** (0.87 g, 36%) as a white solid. $C_{12}H_{23}K_5O_{30}W_2$ (1210.5): calcd. C 12.3, H 1.7; found C 11.9, H 1.9. IR (KBr): $\nu_{as}(C=O)$ = 1731 s, 1654 vs; $\nu_s(C=O)$ = 1437 m, 1387 s, 1335 m; ν(W=O) = 950 s; ν(O–O) = 837 s; $\nu_{as}W(O–O)$ = 637 s; $\nu_sW(O–O)$ = 571 m cm^{-1}. ^1H NMR (500 MHz): δ = 2.86 (d, J = 15.0 Hz, 1 H, CH_2), 2.83 (d, J = 15.0 Hz, 1 H, CH_2), 2.76 (d, J = 16.5 Hz, 1 H, CH_2), 2.72 (d, J = 15.5 Hz, 1 H, CH_2) ppm. ^{13}C NMR (125 MHz): δ = 189.0, 187.4 $(CO_2)_\alpha$, 179.3, 178.4 $(CO_2)_\beta$, 88.1, 85.6 (≡CO), 48.5, 47.3 (=CH_2) ppm.

Preparation of $K_3[W_2O_3(O_2)_4(OH)]\cdot H_2O$ (2): Potassium tungstate (4 mmol), prepared in situ as above, and citric acid (0.92 g, 4.4 mmol) were dissolved in 5 mL of water and an excess of 30% hydrogen peroxide (1 mL) was added dropwise in an ice-bath. Potassium hydroxide was added to give a light-yellow solution of pH 7. Colorless crystals were obtained from EtOH/H_2O solution after cooling in a refrigerator for several weeks and these were washed with ethanol to give **2** (8.2 mg, 0.5%) as a white solid. IR (KBr): ν(OH) = 3641 vs, 3409 vs; ν(W=O) = 970 s, 928 vs; ν(O–O) = 841 vs; ν(W–O–W) = 703 s; $\nu_{as}W(O–O)$ = 605 s; $\nu_sW(O–O)$ = 564 s cm^{-1}.

Preparation of $K_4[W_2O_2(O_2)_4\{(R,R)\text{-tart}\}]\cdot 3H_2O$ (3): An aqueous solution of (*R*,*R*)-tartaric acid (0.36 g, 2.4 mmol) and an excess of 30% hydrogen peroxide (1 mL) were added slowly to a stirred solution of potassium tungstate (4.0 mmol) in an ice-bath. Hydrochloric acid was then added to adjust the solution to pH 3. To induce precipitation, 95% ethanol solution was added dropwise until a permanent turbidity was obtained. The ethanol solution was kept in a refrigerator for several days to give colorless crystals, which were filtered and washed with ethanol to give **3** (0.60 g, 34%) as a white solid. $C_4H_8K_4O_{19}W_2$ (884.2): calcd. C 5.4, H 0.9; found C 5.0, H 0.7. IR (KBr): $\nu_{as}(C=O)$ = 1642 vs, 1612 vs; $\nu_s(C=O)$ = 1382 s; ν(W=O) = 926 s; ν(O–O) = 844 m; $\nu_{as}W(O–O)$ = 627 m; $\nu_sW(O–$

Table 3. Crystal data and structure refinement for $K_5[WO(O_2)_2(Hcit)H(Hcit)(O_2)_2OW]\cdot 6H_2O$ (**1**), $K_3[W_2O_3(O_2)_4(OH)]\cdot H_2O$ (**2**), and $K_4[W_2O_2(O_2)_4\{(R,R)\text{-tart}\}]\cdot 3H_2O$ (**3**).

Empirical formula	$C_{12}H_{23}O_{30}K_5W_2$	$H_3O_{13}K_3W_2$	$C_4H_8O_{19}K_4W_2$
Formula mass	1210.5	696.2	884.2
Crystal color, habit		colorless, needle	
Crystal size [mm]	0.45 × 0.09 × 0.07	0.15 × 0.04 × 0.04	0.20 × 0.05 × 0.05
a [Å]	7.9107(4)	8.2899(4)	15.9030(7)
b [Å]	9.4857(5)	13.7073(6)	
c [Å]	11.3471(6)	21.308(1)	7.8151(4)
α [°]	72.517(1)	21.308(1)	7.8151(4)
β [°]	77.767(1)	21.308(1)	7.8151(4)
γ [°]	71.983(1)	21.308(1)	7.8151(4)
V [°]	765.64(7)	2421.3(2)	1976.5(1)
Z	1	8	4
$D_{\text{calcd.}}$ [g cm^{-3}]	2.625	3.819	2.971
$F(000)$	578	2496	1640
Diffractometer		Smart Apex CCD	
Radiation		Mo-K_α (λ = 0.7107 Å)	
Temp. [°C]		23	
Flack parameter[54]			0.03(3)
GOF on F^2	1.02	1.14	1.17
R_1 [$I > 2\sigma(I)$]	0.037	0.049	0.044
R_1 (all data)	0.038	0.051	0.047

O) = 577 m cm^{-1}. ^{1}H NMR (500 MHz): δ = 4.456 (s, 2 H, CH) ppm. ^{13}C NMR (125 MHz): δ = 186.6, 186.2 $(CO_2)_\alpha$, 88.2, 87.0 (≡CO) ppm.

Transformation of $K_2[W_2O_3(O_2)_4(H_2O)_2]\cdot 2H_2O$ (4) into 1: The dimeric peroxotungstate **4** (0.50 g, 0.7 mmol), prepared by the published method,[23] was dissolved in 5 mL of water. Citric acid (0.34 g, 1.5 mmol) was added to this solution followed by a small amount of 30% H_2O_2. The resulting mixture was stirred and the pH adjusted to 4 with potassium hydroxide (1 M). Colorless crystals of **1** (0.28 g, 33%) were obtained after one day in the refrigerator.

Transformation of 4 into 3: Peroxotungstate **4** (0.65 g, 0.94 mmol) in water was added to (R,R)-tartaric acid (0.15 g, 0.56 mmol) in an ice-bath. Hydrochloric acid was added followed by a small amount of 30% H_2O_2 to get a solution of pH 3. The solution was kept in a refrigerator for two days to give colorless crystals of **3** (0.092 g, 11%).

Transformation of $K_4[W_2O_5(Hcit)_2]\cdot 4H_2O$ (6) into 1: A solution of dimeric hydrogendioxocitratotungstate (**6**; 1.79 g, 1.4 mmol), prepared as reported previously,[56] in water was added to excess 30% hydrogen peroxide (1 mL) to give a solution of pH 4. The solution was kept in a refrigerator for two days to afford yellow crystals of **1** (0.94 g, 55%).

X-ray Structure Determination: Diffraction data were collected on a Bruker Smart Apex CCD diffractometer with graphite-monochromated Mo-K_α radiation at 296 K. Further details can be found in Table 3. The structures were solved with SHELXS-97 and refined by full-matrix least-squares procedures with anisotropic thermal parameters for all the non-hydrogen atoms. H-atoms were located from a difference Fourier map. All calculations were performed with the programs SHELXL-97 and SHELXS-97.[57,58]

CCDC-284258 to -284260 contain the supplementary crystallographic data for this paper. These data can be obtained free of charge from The Cambridge Crystallographic Data Centre via www.ccdc.cam.ac.uk/data_request/cif.

Supporting Information (for details see the footnote on the first page of this article): Details of IR spectra, ^{1}H NMR spectra, and thermogravimetric analyses.

Acknowledgments

We thank the Ministry of Science & Technology (2005CB221408, 2001CB108906) and the National Natural Science Foundation of China (20571061, 20021002, 20423002) for their generous support of this research.

---

[1] K. Sato, M. Aoki, R. Noyori, *Science* **1998**, *281*, 1646–1647.

[2] B. Tamami, H. Yeganeh, *React. Funct. Polym.* **2002**, *50*, 101–106.

[3] S. E. Jacobson, D. A. Muccigrosso, F. Mares, *J. Org. Chem.* **1979**, *44*, 921–924.

[4] R. Noyori, M. Aoki, K. Sato, *Chem. Commun.* **2003**, 1977–1986.

[5] Y. Ishii, Y. Sakata, *J. Org. Chem.* **1990**, *55*, 5545–5547.

[6] A. J. Bailey, W. P. Griffith, B. C. Parkin, *J. Chem. Soc., Dalton Trans.* **1995**, 1833–1837.

[7] A. Arcoria, F. P. Ballisteri, G. A. Tomaselli, F. D. Furia, G. Modena, *J. Mol. Catal.* **1983**, *18*, 177–188.

[8] A. Arcoria, F. P. Ballisteri, G. A. Tomaselli, *J. Mol. Catal.* **1984**, *24*, 189–196.

[9] J. Hu, R. C. Burns, *J. Mol. Catal. A: Chem.* **2002**, *184*, 451–464.

[10] M. S. Reynolds, K. J. Babinski, M. C. Bouteneff, J. L. Brown, R. E. Campbell, M. A. Cowan, M. R. Durwin, T. Foss, P. O'Brien, H. R. Penn, *Inorg. Chim. Acta* **1997**, *263*, 225–230.

[11] M. Shi, Y. S. Feng, *J. Org. Chem.* **2001**, *66*, 3235–3237.

[12] W. Adam, P. L. Alsters, R. Neumann, C. R. Saha-Möller, D. Sloboda-Rozner, R. Zhang, *J. Org. Chem.* **2003**, *68*, 1721–1728.

[13] A. Arcoria, F. P. Ballistreri, G. A. Tomaselli, *J. Org. Chem.* **1986**, *51*, 2374–2376.

[14] D. V. Deubel, J. Sundermeyer, G. Frenking, *Eur. J. Inorg. Chem.* **2001**, 1819–1827.

[15] C. D. Valentin, P. Gisdakis, I. V. Yudanov, N. Rösch, *J. Org. Chem.* **2000**, *65*, 2996–3004.

[16] C. Aubry, G. Chottard, N. Plazzer, J. M. Brégeault, R. Thouvenot, F. Chauvea, C. Huet, H. Ledon, *Inorg. Chem.* **1991**, *30*, 4409–4415.

[17] K. A. Jørgensen, *Chem. Rev.* **1989**, *89*, 431–458.

[18] G. Gelbard, F. Breton, M. Quenard, D. C. Sherrington, *J. Mol. Catal. A: Chem.* **2000**, *153*, 7–18.

[19] Z. W. Xi, N. Zhou, Y. Sun, K. L. Li, *Science* **2001**, *292*, 1139–1141.

[20] P. U. Maheswari, P. de Hoog, R. Hage, P. Gamez, J. Reedijk, *Adv. Synth. Catal.* **2005**, *347*, 1759–1764.
[21] X. Y. Wang, H. C. Shi, S. Y. Xu, *J. Mol. Catal. A: Chem.* **2003**, *206*, 213–223.
[22] R. Stomberg, *J. Less-Common Metals* **1988**, *143*, 363–371.
[23] F. W. B. Einstein, B. R. Penfold, *Acta Crystallogr.* **1964**, *17*, 1127–1133.
[24] N. J. Campbell, A. C. Dengel, C. J. Edwards, W. P. Griffith, *J. Chem. Soc., Dalton Trans.* **1989**, 1203–1208.
[25] T. Ozeki, T. Yamase, *Bull. Chem. Soc. Jpn.* **1997**, *70*, 2101–2105.
[26] W. P. Griffith, B. C. Parkin, A. J. P. White, D. J. Williams, *J. Chem. Soc., Dalton Trans.* **1995**, 3131–3138.
[27] H. Suzuki, M. Hashimoto, S. Okeya, *Eur. J. Inorg. Chem.* **2004**, 2632–2634.
[28] *Polyoxometalate Chemistry* (Eds.: M. T. Pope, A. Müller), Kluwer Academic Publishers, **2001**, pp. 145–149.
[29] O. W. Howarth, *Dalton Trans.* **2004**, 476–481.
[30] M. H. Dickman, M. T. Pope, *Chem. Rev.* **1994**, *94*, 569–584.
[31] D. Chakraborty, M. Bhattacharjee, R. Krätzner, R. Siefken, H. W. Roesky, I. Usón, H. G. Schmidt, *Organometallics* **1999**, *18*, 106–108.
[32] B. Pecquenard, S. Castro-Garcia, J. Livage, P. Y. Zavalij, M. S. Whittingham, R. Thouvenot, *Chem. Mater.* **1998**, *10*, 1882–1888.
[33] W. P. Griffithm, A. M. Z. Slawin, K. M. Thompson, D. J. Williams, *J. Chem. Soc., Chem. Commun.* **1994**, 569–570.
[34] N. M. Gresley, W. P. Griffith, B. C. Parkin, A. J. P. White, D. J. Williams, *J. Chem. Soc., Dalton Trans.* **1996**, 2039–2045.
[35] J. Y. Piquemal, C. Bois, J. M. Brégeault, *Chem. Commun.* **1997**, 473–474.
[36] M. L. Ramos, M. M. Pereira, A. M. Beja, M. R. Silva, J. A. Paixão, V. M. S. Gil, *J. Chem. Soc., Dalton Trans.* **2002**, 2126–2231.
[37] M. L. Ramos, M. M. Calderia, V. M. S. Gil, *J. Chem. Soc., Dalton Trans.* **2000**, 2099–2103.
[38] T. T. Bhengu, D. K. Sanyal, *Thermochim. Acta* **2003**, *397*, 181–197.
[39] M. R. Maurya, M. N. Jayaswal, *J. Chem. Res.* **1988**, 446–447.
[40] R. Stomberg, *Acta Chem. Scand. A* **1970**, *24*, 2024–2036.
[41] J. Flanagan, W. P. Griffith, A. C. Skapski, R. W. Wiggins, *Inorg. Chim. Acta* **1985**, *96*, L23–L24.
[42] A. C. Dengel, W. P. Griffith, R. D. Powell, A. C. Skapski, *J. Chem. Soc., Dalton Trans.* **1987**, 991–995.
[43] A. C. Dengel, W. P. Griffith, R. D. Powell, A. C. Skapski, *J. Chem. Soc., Chem. Commun.* **1986**, 555–556.
[44] H. Glas, M. Spiegler, W. R. Thiel, *Eur. J. Inorg. Chem.* **1998**, 275–281.
[45] D. Bayot, B. Tinant, M. Devillers, *Inorg. Chim. Acta* **2004**, *357*, 809–816.
[46] Z. H. Zhou, S. Y. Hou, H. L. Wan, *Dalton Trans.* **2004**, 1393–1399.
[47] J. A. Brito, M. Gómez, G. Muller, H. Teruel, J. C. Clinet, E. Duñach, M. A. Maestro, *Eur. J. Inorg. Chem.* **2004**, 4278–4285.
[48] R. Stomberg, S. Olson, *Acta Chem. Scand. A* **1985**, *39*, 79–83.
[49] X. B. Shi, C. G. Li, S. H. Wu, J. Chen, G. Y. Xie, *Chin. Sci. Bull.* **1994**, *39*, 1886–1889.
[50] M. Hashimoto, T. Ozeki, H. Ichida, Y. Sasaki, K. Matsumoto, T. Kudo, *Chem. Lett.* **1987**, 1873–1876.
[51] R. Stomberg, *Acta Chem. Scand. A* **1985**, *39*, 507–514.
[52] G. E. Bacon, R. J. Jude, *Z. Kristallogr.* **1973**, *138*, 19–40.
[53] K. Kamata, K. Yamaguchi, S. Hikichi, N. Mizuno, *Adv. Synth. Catal.* **2003**, *345*, 1193–1196.
[54] H. D. Flack, *Acta Crystallogr., Sect. A* **1983**, *39*, 876–881.
[55] R. Stomberg, *Acta Chem. Scand.* **1968**, *22*, 1072–1090.
[56] H. Zhang, H. Zhao, Y. Q. Jiang, S. Y. Hou, Z. H. Zhou, H. L. Wan, *Inorg. Chim. Acta* **2003**, *351*, 311–318.
[57] L. J. Farrugia, *J. Appl. Crystallogr.* **1999**, *32*, 837–838.
[58] G. M. Sheldrick, *SHELXL97 and SHELXS97*, University of Göttingen, Germany, **1997**.

Received: November 13, 2005